

Skeletal Muscle Is an Antigen Reservoir in Integrase-Defective Lentiviral Vector-Induced Long-Term Immunity

Yi-Yu Lin,^{1,2} Ian Belle,^{1,6} Maria Blasi,^{1,2} Min-Nung Huang,¹ Anne F. Buckley,³ Wes Rountree,² Mary E. Klotman,^{1,2} Andrea Cara,^{1,2,4} and Donatella Negri^{1,2,5}

¹Department of Medicine, Duke University Medical Center, Durham, NC 27710, USA; ²Duke Human Vaccine Institute, Duke University Medical Center, Durham, NC 27710, USA; ³Department of Pathology, Duke University Medical Center, Durham, NC 27710, USA; ⁴National Center for Global Health, Istituto Superiore di Sanità, Rome, Italy; ⁵Department of Infectious Diseases, Istituto Superiore di Sanità, Rome, Italy

We previously developed integrase-defective lentiviral vectors (IDLVs) as an antigen delivery system for inducing strong and prolonged immunity in animal models. Here, we examined the association between persistence of antigen expression and durability of immune response. Following a single intramuscular (i.m.) or subcutaneous (s.c.) injection of IDLV delivering GFP in mice, we evaluated antigen expression and inflammation at the site of injection and persistence of antigen-specific T cells at early and late time points. Durable antigen expression was detected up to 90 days only after i.m. immunization. Mononuclear inflammation was evident soon after IDLV injection in both i.m. and s.c. immunized mice, but remained detectable up to 30 days postinjection only in i.m. immunized mice. Similarly, GFP-specific T cells were more persistent in the i.m. immunized mice. Interestingly, GFP⁺ muscle fibers were co-expressing major histocompatibility complex (MHC) class I, suggesting that muscle cells are competent for presenting antigens to T cells *in vivo*. In *in vitro* experiments, we demonstrated that although both primary myoblasts and myocytes present the antigen to GFP-specific T cells through MHC class I, myoblasts are more resistant to Fas-dependent cytotoxic T lymphocyte (CTL) killing activity. Overall, these data indicate that muscle cells may serve as an antigen reservoir that contributes to the long-term immunity induced by IDLV vaccination.

INTRODUCTION

Conventional vaccine approaches, including inactivated and live attenuated pathogens and subunit vaccines, provide protection against several infectious diseases.¹ However, those approaches are not viable options against a variety of infectious pathogens able to evade the immune response, such as HIV-1, tuberculosis, and many others.² Therefore, the development of vaccine platforms that can efficiently protect against more challenging pathogens remains a high priority.

Genetic vaccines, including DNA plasmid and recombinant vector-based approaches, have emerged as alternative and versatile platforms

for antigen delivery in both preventive and therapeutic settings.^{3,4} Compared with subunit-based vaccines intended to induce mainly antibody responses, genetic vaccines induce a more comprehensive and durable immunity, including potent T cell responses.⁵ Among genetic vaccines, viral vectors hold much promise as vaccine platforms, providing durable expression of the antigen and strong and long-term immune responses.^{6–8} Viral-based vaccines have now reached an excellent safety profile and include a variety of recombinant vectors for tailoring the immune response to specific applications. Currently, many of them are under investigation in human trials.⁴ Further elucidation of immune responses preferentially induced by specific viral vectors and how those responses are maintained is required to determine as to which vectors are most effective for vaccination against specific infectious agents.

We have previously shown that integrase-defective lentiviral vectors (IDLVs) are an efficient and safe platform for vaccination.^{9,10} IDLVs are self-inactivating, non-integrating, and non-replicating lentiviral vectors with high transduction efficiency both *in vitro* and *in vivo*. In contrast with parental integrating lentiviral vectors, IDLVs are produced by incorporating a mutated form of the integrase protein, preventing integration and avoiding the risk for insertional mutagenesis.¹¹ In the absence of integration, transgene expression is from the unintegrated circular forms of the vector, which are maintained as DNA episomes in non-proliferating target cells.^{12–14} Only the transgene of interest is expressed from episomal IDLV in the absence of any other parental viral product.

Received 6 February 2020; accepted 10 March 2020;
<https://doi.org/10.1016/j.omtm.2020.03.008>

⁶Present address: Charles River Discovery Services, Morrisville, NC 27560, USA

Correspondence: Donatella Negri, Department of Medicine, Duke University Medical Center, 2 Genome Court, Durham, NC 27710, USA.

E-mail: donatella.negri@duke.edu

Correspondence: Andrea Cara, Department of Medicine, Duke University Medical Center, 2 Genome Court, Durham, NC 27710, USA.

E-mail: andrea.cara1@duke.edu



IDLV represents an effective antigen delivery and gene-editing platform.^{10,15} In particular, IDLV vaccination has been shown to elicit robust antigen-specific immune responses in mice^{16–19} and non-human primates (NHPs),^{20,21} as well as in humans in anti-cancer immune therapy.²² We demonstrated that episomal IDLV persists at the injection site up to several months after intramuscular (i.m.) immunization,^{16,23} supporting the association between duration of antigen expression by IDLV and induction of strong and persistent immunity, as previously described for other vaccines.^{24,25} Importantly, we have recently demonstrated that IDLV persistence *in vivo* correlates with the induction of STING-independent CD8⁺ T cell responses.²⁶

In the present study, we explored the association between duration of antigen expression and induction of durable immune responses by focusing on the role of the cells transduced by IDLV following i.m. or subcutaneous (s.c.) immunization. We demonstrated that after i.m. immunization, the antigen expression persists up to 90 days in IDLV-transduced muscle cells. We also demonstrated that although primary muscle cells can efficiently present the antigen to T cells via major histocompatibility complex (MHC) class I, they showed a low sensitivity to cytotoxic T lymphocyte (CTL)-induced cytotoxicity mediated by FasL. In the absence of a robust inflammatory response, IDLV persists and continuously expresses the encoded antigen, which in turn maintains the vaccine-induced immune response.

RESULTS

Antigen Persists at the Site of Injection after i.m. Immunization with IDLV

We previously reported the persistence of vector DNA in the skeletal muscle of both mice and macaques immunized with IDLV up to 6 months post-immunization.^{21,27} To investigate the role of antigen persistence in the generation of long-term immunity induced by immunization with IDLV, we injected mice either i.m. or s.c. with IDLV-GFP, phosphate-buffered saline (PBS), or left them untreated. Animals were sacrificed at 3, 30, or 90 days after a single vaccination, and the expression of GFP at the injection site and in draining lymph nodes (dLNs) was assessed by confocal microscopy (Figure 1). Three days after immunization, GFP expression was detected at the injection site in both muscle and in skin (Figures 1Aa, 1Ab, and 1Bj), but remained detectable at day 30 after immunization only in muscle (Figures 1Ad and 1Ae), where it persisted at lower levels up to 90 days postinjection (Figures 1Ag and 1Ah). In contrast, 30 days after s.c. immunization, GFP expression was undetectable in the skin (Figure 1Bl). Muscle and skin sections from PBS-injected mice were used as negative controls (Figures 1Ac, 1Af, 1Bi, 1Bk, and 1Bm). As expected, GFP-expressing cells were evident in dLNs 3 days after i.m. and s.c. immunization with IDLV-GFP (Figures 1Cn and 1Cp, respectively), whereas no GFP expression was detected in LNs 30 days postinjection (Figures 1Cq and 1Cs). dLNs from PBS-injected mice were used as negative controls (Figures 1Co and 1Cr). By using the ImageJ software on confocal microscopy images (Figure 1D), a higher GFP expression was observed in dLNs from the s.c. group compared with i.m., likely because of the higher number of resident antigen-pre-

sented cells (APCs) transduced with the injected vector in the skin compared with the muscle.

These results indicate that GFP is expressed in dLNs early after IDLV-GFP injection, regardless of the route of immunization, whereas IDLV-transduced skeletal muscle cells continue to express the encoded antigen for several weeks after i.m. injection.

IDLV Immunization Induces Detectable Cellular Infiltration at the Site of Injection

Inflammation at the injection site was assessed by routine H&E histology at 3, 30, and 90 days after injection. We observed similar levels of mononuclear inflammation at the injection site early postinjection in animals receiving either IDLV-GFP or PBS (Figure 2A), suggesting that early inflammation at the injection site is primarily due to the injection itself. Thirty days postinjection, inflammation persisted at very low levels in the muscle of animals i.m. injected with IDLV-GFP, whereas inflammation had resolved in animals receiving s.c. injections of IDLV-GFP or PBS (Figure 2B). We characterized the cellular infiltrate at the site of injection after i.m. injection of IDLV-GFP or PBS by immunohistochemistry. T cells and F4/80⁺ macrophages were detectable in the inflammation infiltrate 30 days post-vaccination (Figure 2C). These results suggest that immunization with an IDLV-based vaccine induces transient inflammation at the injection site, and that persistence of transduced cells in muscle expressing the vaccine antigen is associated with foci containing small numbers of macrophages and T cells at later time points.

i.m. Immunization Provides a More Durable Antigen-Specific Immune Response Than s.c. Immunization

In order to assess and compare the durability of the GFP-specific T cell response after i.m. or s.c. vaccination with IDLV-GFP, we harvested splenocytes from IDLV-immunized mice 30 and 90 days after immunization and measured the magnitude of functional GFP-specific CD8⁺ T cells by interferon γ (IFN γ) Enzyme-Linked Immunospot (ELISpot) assay. GFP-specific T cell response, measured as spot-forming cells (SFCs) per million splenocytes and as a percentage of GFP-specific T cells present in the sample calculated as a ratio between GFP-SFC and concanavalin A (ConA)-SFC (Figure 3), could be detected 90 days after vaccination regardless of the injection route. These results confirm published data showing that IDLV induces a long-lasting and functional antigen-specific immune response after a single vaccination.^{18,27} However, in s.c. immunized mice, the magnitude of the response decreased more rapidly compared with i.m. injected mice ($p < 0.05$; Figure 3B). Conversely, there was no significant decline in the i.m. immunized mice, suggesting that the injection route and the persistent antigen expression from the transduced target cells play a role in the durability of IDLV-induced immunity.

GFP-Positive Muscle Fibers *In Vivo* Express MHC Class I

To further understand the role of transduced muscle cells in the durability of IDLV-induced immunity, we assessed whether we could detect the expression of MHC class I molecules in muscle from naive,

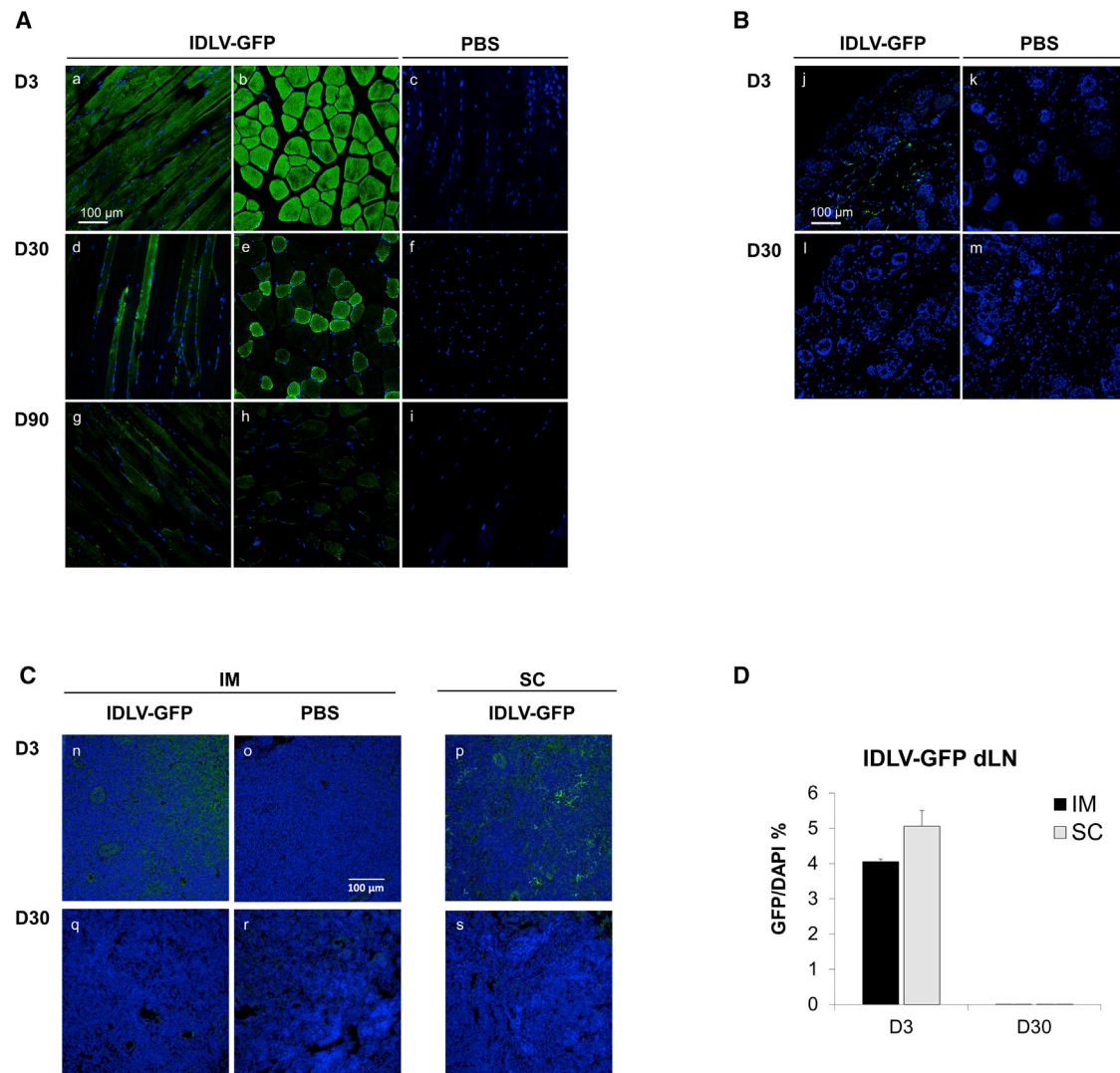


Figure 1. Persistent GFP Expression at the Injection Site after Intramuscular Immunization with IDLV-GFP

BALB/c mice injected with IDLV-GFP or PBS using either the intramuscular (i.m.) or subcutaneous (s.c.) route were sacrificed at different time points. Skeletal muscle and skin sections were stained for GFP (green) and DAPI (blue). (A and B) Representative confocal microscopy images of muscle after i.m. immunization (A) and skin after s.c. immunization (B) are shown at 3, 30, and 90 days (D3, D30, and D90). Longitudinal (a, d, and g) and cross-sectional images (b, e, and h) of skeletal muscle are shown. (C) Representative confocal microscopy images of dLNs stained for GFP and DAPI from mice injected either i.m. (n and q) or s.c. (p and s) with IDLV-GFP or PBS (o and r). (D) Quantitative analysis of GFP expression evaluated using the ImageJ software, shown as % GFP⁺ area on DAPI⁺ area in dLNs from IDLV-GFP-immunized mice (n = 3 for each group).

PBS-injected, and IDLV-GFP-immunized mice. MHC class I expression was detected by immunofluorescence on the sarcolemma of scattered muscle fibers (Figure 4A). No difference between naive and IDLV-GFP-injected mice was observed either at 3 or 30 days after IDLV injection, suggesting that MHC class I expression was not substantially modified upon vaccination with IDLV (Figure 4B). Double staining for MHC class I and GFP revealed expression of MHC class I in GFP-positive fibers at 3 and 30 days post-immunization (Figure 4C), suggesting that muscle cells can present the antigen to T cells through MHC class I.

Primary Myoblasts and Myocytes Can Present Antigen to Specific Effector T Cells

To evaluate the ability of skeletal muscle cells to present the antigen to effector T cells, we performed *in vitro* co-culture experiments using primary murine muscle cells at different stages of differentiation. Myoblasts isolated from 3-week-old BALB/c mice were cultured either in the absence or presence of differentiation stimuli to allow differentiation into myocytes (Figure 5A). MHC class I expression was detected by immunofluorescence in both myoblasts and myocytes (Figure 5B). Next, we assessed the ability of primary myoblasts

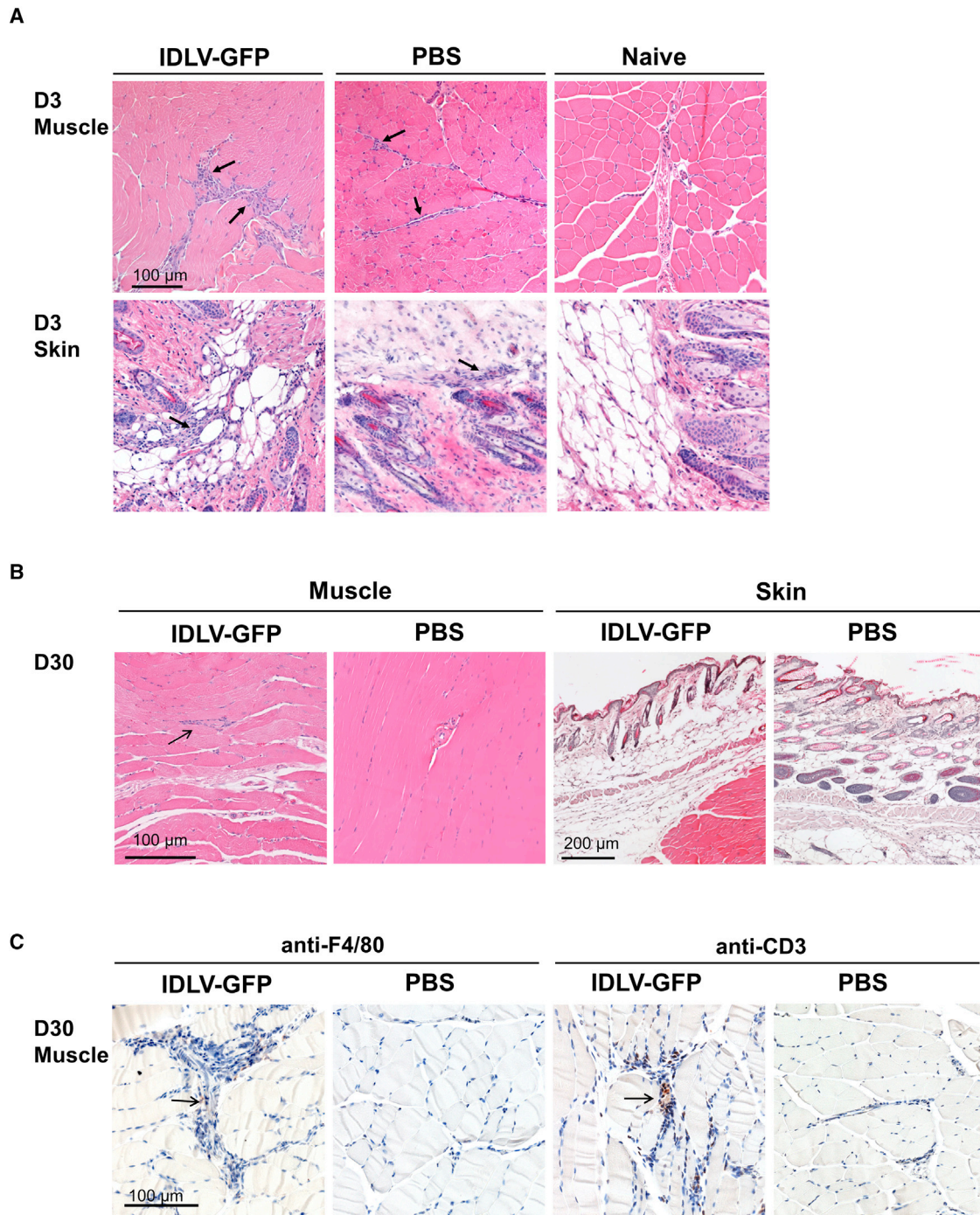


Figure 2. IDLV Immunization Induces Mononuclear Cellular Infiltration

(A) H&E staining of skeletal muscle and skin sections from mice injected i.m. or s.c., respectively, with IDLV-GFP, PBS, or left untreated (naive) at 3 days (D3) postinjection. (B) H&E staining of muscle and skin tissues at 30 days (D30) after i.m. or s.c. injection, respectively, with IDLV-GFP or PBS. Arrows indicate foci of inflammatory cells. (C) F4/80 and CD3 as macrophage and T cell markers, respectively, were used to stain muscle sections from mice injected with IDLV-GFP or PBS at 30 days after injection. Arrows indicate macrophages and T cells within the cellular infiltration.

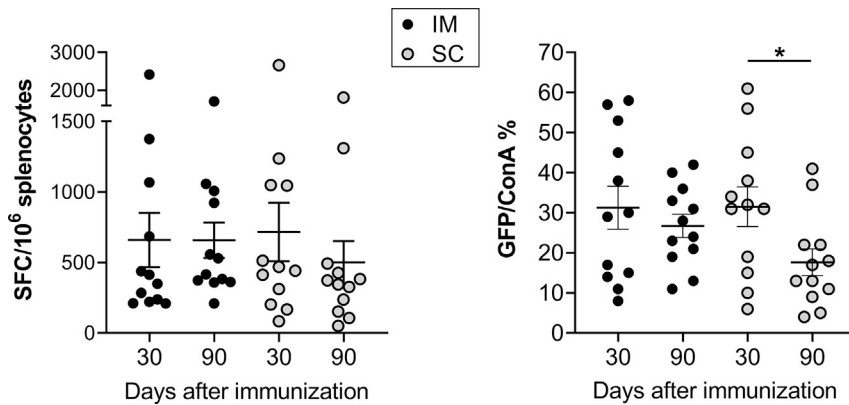


Figure 3. GFP-Specific T Cell Response Is More Persistent after i.m. Immunization

GFP-specific T cells from mice immunized with IDLV-GFP were evaluated in splenocytes by IFN- γ ELISpot assay at 30 and 90 days after i.m. or s.c. injection. Cells were stimulated overnight with H-2d-restricted GFP 9-mer peptide HYLSTQSAI (GFP), concanavalin A (ConA), or left untreated. Data are expressed as numbers of specific spot-forming cells (SFCs) per million cells (left panel) and as % of GFP-specific SFCs normalized per ConA-induced SFCs (right panel). Data from three different experiments ($n = 12$) are shown. Black lines represent the mean and SEM. Asterisk indicates a statistically significant difference between the indicated groups ($*p < 0.05$).

and myocytes to present the antigen to antigen-specific effector T cells by IFN- γ ELISpot assay. Myoblasts and myocytes were pulsed with either MHC I-restricted GFP peptide or transduced with the integrase competent lentiviral vector (LV)-GFP and then co-cultured with splenocytes isolated from mice previously immunized with IDLV-GFP or injected with PBS, as depicted in details in Figure 5C. Both GFP peptide-pulsed and LV-GFP-transduced myoblasts and myocytes induced IFN- γ production by GFP-specific splenocytes (Figure 5D). GFP-pulsed splenocytes were used as a positive control of the assay. Treatment with anti-MHC class I antibody blocked the production of IFN- γ by antigen-specific T cells, demonstrating that primary muscle cells present the antigen to effector T cells through MHC class I (Figure 5D).

Myoblasts Are Resistant to CTL-Induced Cytotoxicity Mediated by the Fas/FasL Pathway

CTLs play an important role in the clearance of cells expressing foreign antigens, such as viral-infected cells or tumor cells. Because both primary myoblasts and myocytes are capable of presenting antigens to T cells, they could be susceptible to killing by antigen-specific CTLs. To address this, we performed a lactate dehydrogenase (LDH) assay to measure CTL-induced cytotoxicity using splenocytes isolated from either IDLV-GFP- or PBS-injected mice activated *in vitro* with MHC class I-restricted GFP peptide for 3 days and then co-cultured with GFP peptide-pulsed primary muscle cells or the H-2d-matched P815 cell line. After 8 h of incubation, the activated antigen-specific T cells successfully killed GFP-positive myocytes and control P815 cells but demonstrated limited or no killing of myoblasts (Figure 6A).

It has been shown that the Fas/FasL signaling pathway is linked to CTL-induced apoptosis.²⁸ We therefore assessed the expression of Fas in cultured primary myoblasts and myocytes by confocal microscopy (Figure 6B). Both cell types expressed Fas, with the myocytes having higher Fas expression, as quantified by flow cytometry (Figure 6C). Interestingly, after transduction with LV-GFP, we observed a decrease in the level of Fas expression in myocytes, although it was still higher compared with myoblasts (Figure 6C). We therefore investigated whether primary myoblasts and myocytes could be killed

following treatment with low and high doses of FasL. Trypan blue staining was performed to assess cell death following recombinant FasL protein treatment. As shown in Figure 6D, the higher dose of FasL (2 $\mu\text{g}/\text{mL}$) induced cytotoxicity of primary myocytes but had no effect on primary myoblasts (Figure 6D). Splenocytes used as positive control showed the highest sensitivity to FasL-induced cell death, evident even at the lowest dose of FasL (1 $\mu\text{g}/\text{mL}$). It has been shown that serum deprivation induces apoptosis in some cell lines.^{29,30} Because primary myoblasts are maintained in high percentage of serum, we decided to remove the serum from the culture during the treatment with FasL to facilitate the cell death. Indeed, when the same assay was performed using serum-free medium, an increase of cytotoxicity was evident in myocytes showing dose-dependent cytotoxicity (Figure 6D), but not in myoblasts, confirming that myoblasts are resistant to CTL-mediated cytotoxicity induced through the Fas/FasL pathway.

To address this further, we overexpressed Fas in primary myoblasts using a lentiviral vector expressing Fas fused to the GFP protein (LV-Fas/GFP), as evaluated by flow cytometry (Figure 7A). Treatment of LV-Fas/GFP-transduced myoblasts with FasL (2 $\mu\text{g}/\text{mL}$) induced cell death in a high percentage of GFP⁺ cells (Figure 7B). These results demonstrated that overexpression of Fas partially overcomes the resistance to FasL-mediated cytotoxicity in myoblasts.

To confirm Fas expression on muscle cells *in vivo*, we assessed its expression on muscle tissue at days 3 and 30 after i.m. injection with IDLV-GFP or PBS. As shown in Figure 8, similar levels of Fas expression were detected in muscle fibers from both PBS- and IDLV-injected mice and at both early and late time points after the injection.

DISCUSSION

Several studies by our group and others have demonstrated that IDLV-based vaccines administered via different routes induce strong and persistent cellular and humoral antigen-specific immunity.^{17,19,20,26,31,32} The IDLV-delivered transgene has been shown to persist at the injection site up to several months after

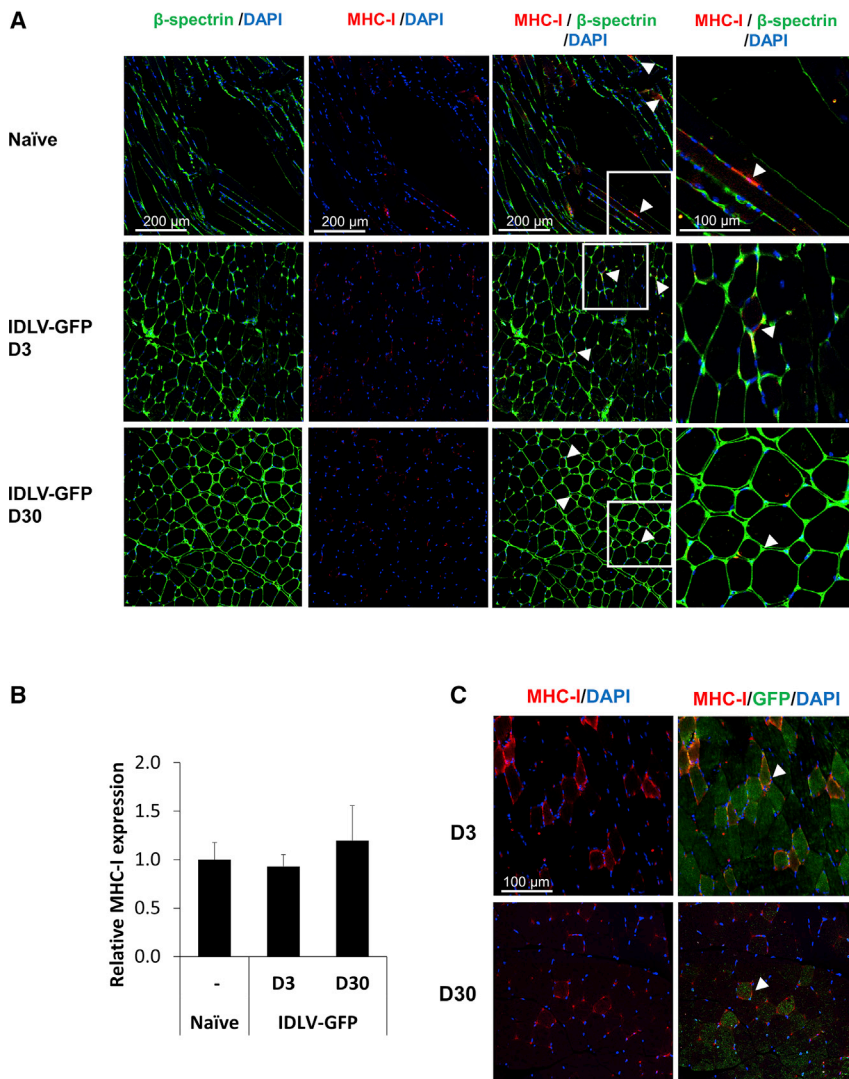


Figure 4. Baseline MHC Class I Expression in Muscle Is Not Modified by IDLV Injection

(A) Muscle from naïve and IDLV-GFP-immunized mice 3 days (D3) and 30 days (D30) postinjection was stained with the cell membrane marker beta-spectrin (green), MHC class I (red), and DAPI (blue) as nuclear staining. The right panels show MHC class I-positive area (white arrowheads) at higher magnification (far right panels). (B) MHC class I expression was quantified using ImageJ software (n = 3 for each group). Error bars represent the SD of three different samples. (C) Representative confocal images of muscle from IDLV-GFP-immunized mice at 3 and 30 days post-injection stained for GFP (green), MHC class I (red), and DAPI (blue). Arrowheads indicate MHC class I and GFP double-positive cells.

immunization both as DNA^{16,17,33} and mRNA.²¹ In this work, we focused our attention on the protein expression to directly associate the antigen production with the persistence of immune response induced by IDLV vaccine.

We showed that IDLV-transduced muscle cells continue to produce the antigen up to 3 months after a single i.m. immunization, demonstrating the ability of IDLV to continuously express a non-self-antigen *in vivo*. Conversely, s.c. immunization resulted in only transient detection of GFP-expressing cells in the skin early postimmunization. These results are in line with a previous report showing IDLV disappearance following s.c. injection,³⁴ likely because of the nature of the cells transduced by the vector following s.c. injection, including dendritic cells (DCs) that migrate to the dLNs following vaccination.^{35–37}

Both the s.c. and i.m. routes elicited GFP-specific immune responses, as indicated by the number of GFP-specific IFN γ -producing T cells

detected at 30 days after injection. Indeed, it is well known that the initiation of the immune response after vaccination occurred in dLNs, where the antigen, directly migrated through lymphatic vessels or carried by APCs present at the injection site, is processed and presented by APCs to naïve T cells.³⁷ We clearly showed the presence of GFP-expressing cells in dLNs after i.m. and s.c. immunization at 3 days, indicating that the antigen presentation to naïve T cells occurred in dLNs and is responsible for the induction of the antigen-specific immunity observed in both i.m. and s.c. immunized mice. However, although the immune response induced by i.m. injection of IDLV-GFP persisted at similar levels at day 90 post-immunization, a significant decline was observed from days 30 to 90 in the s.c. immunized mice, suggesting that the IDLV-transduced target cells might play a role in the persistence of IDLV-induced immunity. We therefore focused our attention on understanding the role of muscle cells and

questioned whether the prolonged antigen expression observed in muscle tissue is associated with the maintenance of long-term immunity following IDLV immunization, and if so, why the antigen-expressing muscle cells are not eliminated by antigen-specific CTLs.

Analysis of the cellular infiltrate after i.m. and s.c. injection with IDLV-GFP demonstrated the presence of a detectable local inflammation, mainly due to the injection *per se*, as demonstrated by the similar levels of inflammation in tissues from PBS-injected mice. The inflammation resolved completely by 30 days after injection in the skin and partially in the IDLV-injected muscle, whereas infiltrating CD3⁺ T cells and macrophages were still focally evident. Following on our earlier studies showing that intravenous injection of IDLV generated weak and transient innate responses characterized by low levels of inflammatory cytokines and chemokines and transient DC maturation,²⁶ here we provide evidence that i.m. IDLV immunization induces transient and localized inflammation that results in

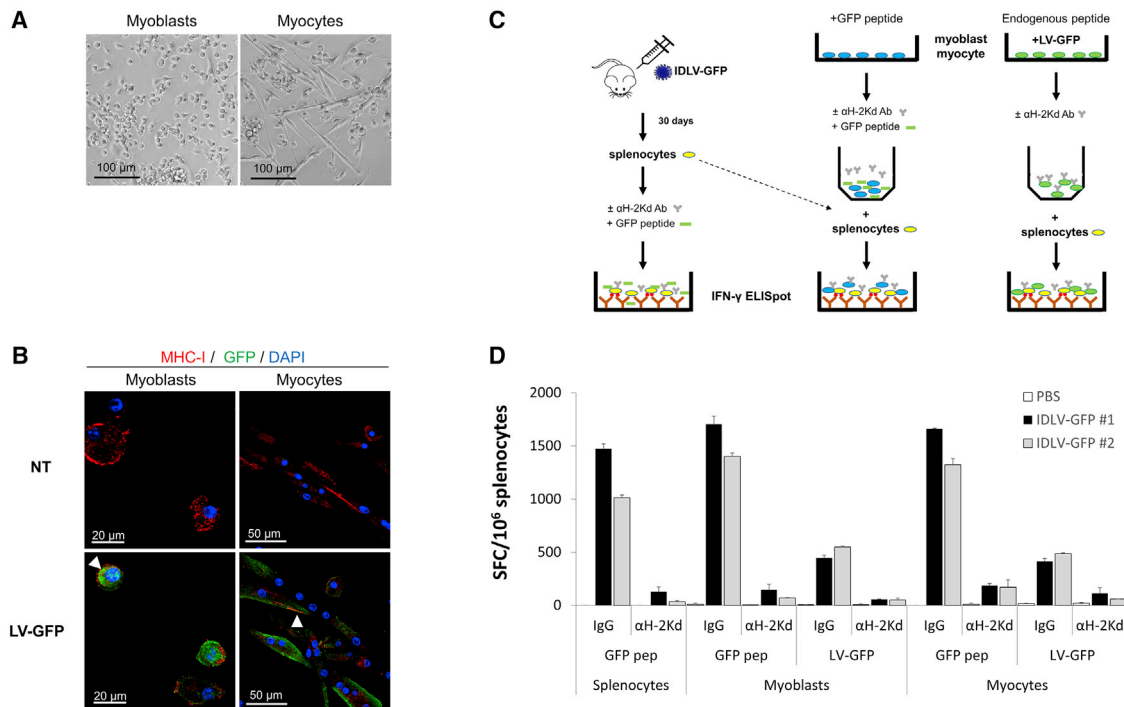


Figure 5. Primary Myoblasts and Myocytes Present the Antigen to Specific Effector T Cells through MHC Class I

(A) Light microscopy images of primary myoblasts purified from 3-week-old BALB/c mice and after differentiation into myocytes. (B) Confocal images of myoblasts and myocytes transduced with LV-GFP or non-transduced (NT), stained for MHC class I (red), GFP (green), and DAPI (blue). White arrowheads indicate MHC class I expression on GFP-positive cells. (C) Layout of the experiment performed to demonstrate the ability of primary muscle cells to stimulate specific T cells. Primary myoblasts and myocytes were either pulsed with H-2d-restricted GFP 9-mer peptide HYLSTQSAL or transduced with LV-GFP and treated with anti-H-2d antibody or an unrelated IgG and then co-cultured with splenocytes from IDLV-GFP- or PBS-injected mice in the ELISpot plate. (D) The stimulation of GFP-specific T cells was assessed by IFN- γ ELISpot assay. Splenocytes pulsed with GFP peptide were used as a positive control of the assay. Results from a representative experiment are shown. Data are expressed as specific spot-forming cells (SFCs) per million splenocytes. Error bars represent the SD of duplicates.

preservation of the antigen, eventually leading to an efficient and durable immunity. In line with these data, it has been shown that among the different serotypes, the most potent adenoviral vectors, in terms of immunity induced after vaccination, are those that induce low innate immunity, providing a more persistent antigen expression.²⁵ All of these data further support the role of the antigen persistence in the generation of durable immune responses.²⁴

To investigate the interplay between immune and muscle cells in the setting of i.m. immunization with IDLV, we assessed the expression of MHC class I molecules in muscle cells early after injection and at later time points. MHC class I molecules, expressed on the cell surface, present peptide fragments to the T cell receptor (TCR) on CD8⁺ T cells, triggering a specific immune response to non-self-antigens.³⁸ Most nucleated cells express MHC class I, although the amount of MHC class I on the cell surface varies among cell types and under different inflammatory conditions. In particular, under normal physiological conditions, muscle fibers were reported to express low or undetectable MHC class I.³⁹ However, MHC class I can be strongly upregulated in pathological conditions, especially in inflammatory muscle diseases, such as myositis.^{40,41} In the present study, we

detected scattered MHC class I expression on muscle fibers, which suggests that although muscle cells have the potential to express MHC class I, not all muscle fibers are expressing MHC class I at the same time. Interestingly, after immunization with IDLV-GFP, we observed co-expression of MHC class I and GFP in muscle cells, suggesting that GFP-expressing muscle cells could contribute toward the maintenance of the immune response by interacting with infiltrating T cells through MHC class I. By large-scale image scanning and quantitative analysis, we did not find a significant difference in the MHC class I expression in muscle tissue between naive, PBS-injected, or IDLV-vaccinated mice. Similar MHC class I expression patterns were observed in muscle tissues harvested at early and late time points after immunization, indicating that IDLV injection did not induce upregulation of MHC class I.

To recapitulate the interplay between muscle cells and T cells *in vivo*, we set up an *in vitro* co-culture system between splenocytes from IDLV-GFP-immunized mice and primary myoblasts or myocytes isolated from the skeletal muscles of naive BALB/c mice. We showed that murine-derived primary myoblasts and myocytes constitutively expressed MHC class I and efficiently presented the antigen to

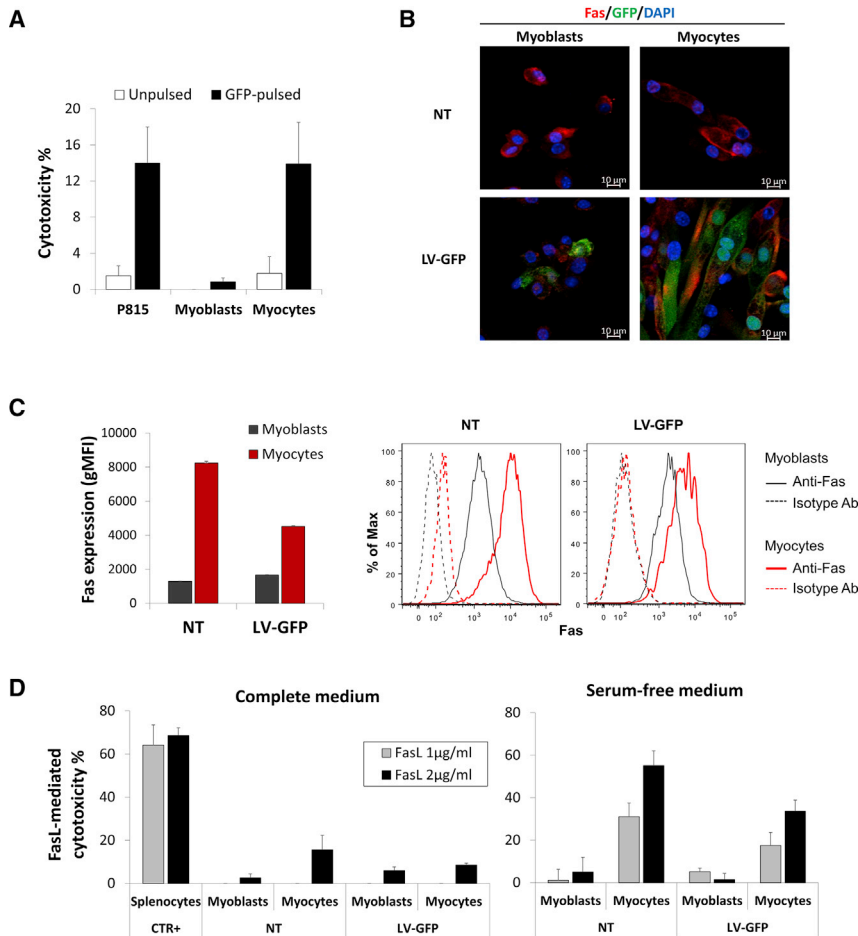


Figure 6. Myoblasts, but Not Myocytes, Are Resistant to CTL-Induced Cytotoxicity

(A) LDH assay was performed to assess the cytotoxicity mediated by specific CTLs. Splenocytes from IDLV-GFP-immunized mice were activated *in vitro* for 3 days with GFP peptide and then co-cultured for 8 h with myoblasts and myocytes pulsed with GFP peptide or left untreated. P815 cell line pulsed or not with GFP peptide was used as a positive control of the assay. Data are expressed as mean % specific cytotoxicity \pm SD of three different experiments assessed at E:T ratio of 80:1. (B) Fas expression evaluated by confocal microscopy on myoblasts and myocytes before (NT) and after transduction with LV-GFP. Anti-Fas (red) and anti-GFP (green) antibodies were used. (C) Fas expression on myoblasts and myocytes by flow cytometry. Data in (C) are expressed as specific geometric mean fluorescence intensity (gMFI \pm SD) from three different experiments after subtraction of the isotype-treated samples gMFI. A representative experiment of analysis by flow cytometry is shown. (D) FasL-His recombinant protein (1 and 2 μ g/mL) and anti-His Ab were used to induce cytotoxicity on splenocytes, myoblasts, and myocytes using either complete medium (left) or medium without serum (right). FasL-induced cell death was measured by trypan blue staining and expressed as mean % cytotoxicity \pm SD of three different experiments.

antigen-specific effector T cells through MHC class I. This is in line with previous *in vitro* studies demonstrating that human myoblasts can form a functional immunological synapse with T cells, by expressing MHC class I or class II molecules, thus acting as nonprofessional APCs.⁴¹ Interestingly, we showed that only myocytes were susceptible to antigen-specific CTLs, whereas myoblasts demonstrated resistance to CTL-induced cytotoxicity.

There are two major pathways that CTL uses to eliminate target cells: perforin-mediated and via Fas/FasL signaling.²⁸ Although perforin-mediated killing is a fast-acting reaction, killing mediated by Fas/FasL-based interaction requires a longer time.⁴² In our study, we detected cytotoxicity in myocytes, but not in myoblasts, only after 8 h of co-culture with splenocytes from GFP-immunized mice, suggesting that CTL-induced cytotoxicity in myocytes uses mainly the Fas/FasL signaling pathway. Following FasL treatment, we observed the killing of myocytes, but not myoblasts, confirming that myoblasts are resistant to CTL-mediated cytotoxicity. Of note, to induce high levels of cytotoxicity in myocytes, the use of a more stringent condition such as serum-free medium was necessary, suggesting that also primary myocytes have a constitutively low sensitivity to FasL-mediated cytotoxicity. In a previous study, primary Fas-expressing myo-

blasts transduced with a retroviral vector to express functional FasL underwent apoptosis only during differentiation in myocytes.⁴³ This is in line with our results, suggesting that myoblasts are naturally resistant to Fas/FasL-induced cytotoxicity, providing an evasion mechanism against CTL activity. Interestingly, we provided evidence that Fas expression was upregulated during differentiation into myocytes, which may link to FasL-induced cell death in myocytes compared with myoblasts, and that myoblasts overexpressing Fas after LV-Fas transduction increased their sensitivity to FasL-mediated cytotoxicity.

In summary, we have demonstrated that following *i.m.* immunization with IDLV, the production of the antigen in muscle cells persisted for several weeks, although a reduction in the amount of antigen produced was evident over the course of 3 months after a single immunization. These data are in agreement with our previous report showing a decrease in the amount of vector in the injected muscle over time,¹⁶ likely due to physiological cell turnover and the modest local CTL activity. Here, by combining the features of the vector with those related to the muscle physiology, we elucidated mechanisms underlying the efficient induction of immune response induced by IDLV-based vaccine. In particular, the moderate inflammation following IDLV injection, including the presence of *i.m.* T cells and macrophages, together with the scattered but constitutive expression of both MHC class I and Fas in muscle fibers and the constitutive resistance of muscle cells to cell death, likely contribute to prolonged stimulation of the specific immune response in combination with low

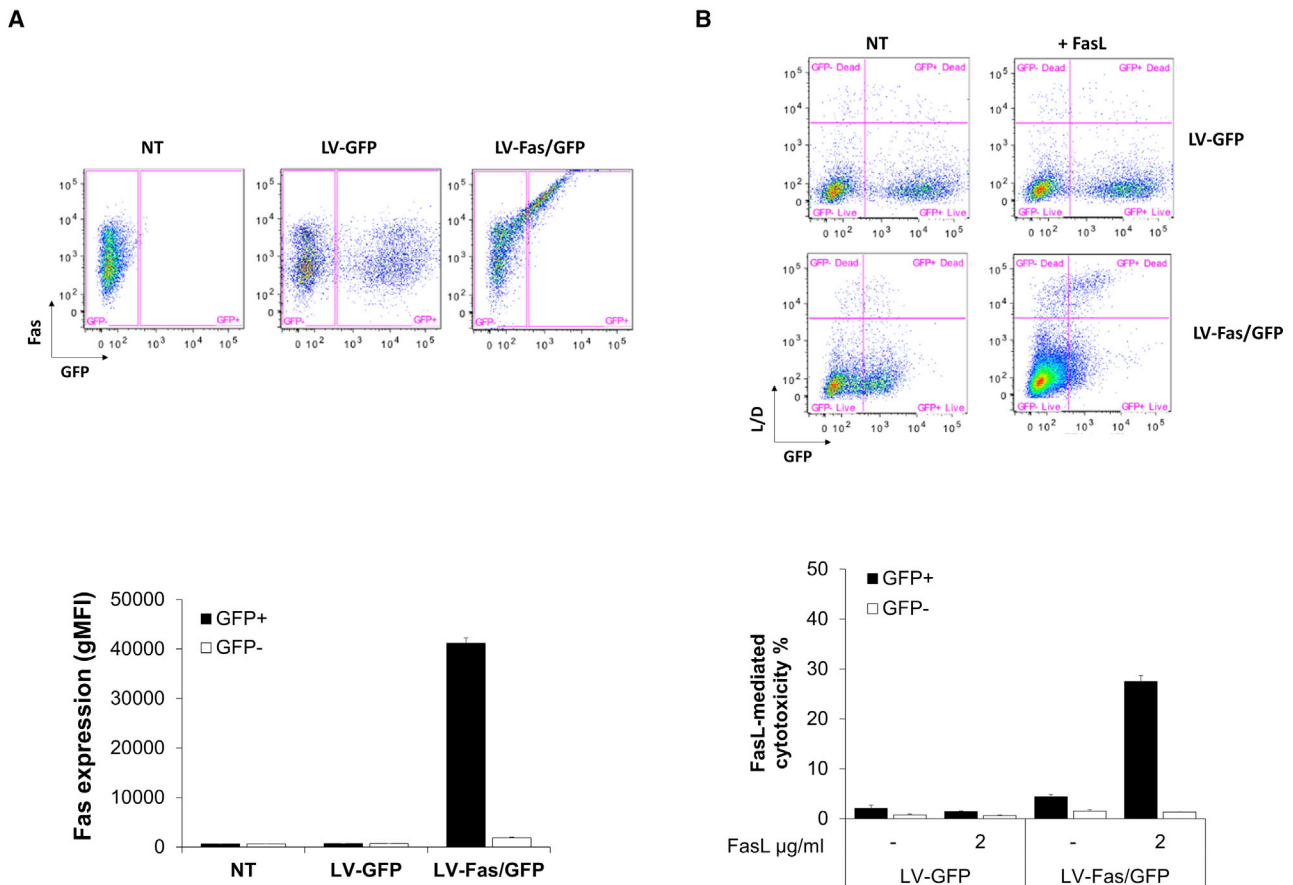


Figure 7. Overexpression of Fas in Myoblasts Resulted in Increased FasL-Mediated Cytotoxicity

(A) Fas expression on myoblasts transduced with LV-GFP, LV-Fas/GFP, or NT was evaluated by flow cytometry. Data are expressed as gMFI. (B) FasL-His recombinant protein (2 µg/mL) and anti-His Ab were used to induce cytotoxicity in myoblasts transduced with LV-GFP or LV-Fas/GFP. FasL-induced cell death, quantified using a live/dead (L/D) stain by flow cytometry, is expressed as mean % cytotoxicity ± SD of triplicates. Flow cytometry analyses of a representative experiment are shown.

levels of local CTL-mediated cytotoxicity. Of note, the persistent antibody response observed in NHPs immunized i.m. with IDLV delivering HIV envelope as a secreted antigen strongly suggested that the continuous release of the antigen from muscle cells contributes also to the long-term IDLV-induced humoral immunity.^{20,21}

Overall, our findings indicate that skeletal muscle cells function as an antigen reservoir for the maintenance of the long-term immunity induced by IDLV.

MATERIALS AND METHODS

Plasmids and Lentiviral Vectors Production

The SIV-based self-inactivating lentiviral transfer vector expressing EGFP (pGAE-CMV-GFPW), the IN-defective packaging plasmid pAd-D64V, and the Envelope plasmid pMD.G producing the pseudotyping vesicular stomatitis virus envelope glycoprotein G (VSV.G) have been previously described^{21,23} and were used for IDLV-GFP production. The lentiviral transfer vector codifying for murine Fas and GFP fusion protein (pLV-mFas-GFPspark) was obtained from

Sino Biological (Wayne, PA, USA). The integrase competent lentiviral vector LV-GFP used for *in vitro* assays was produced by using the IN-competent packaging plasmid pAd-SIV3⁺.²³ For production of recombinant IDLV-GFP and LV-GFP, 3.5×10^6 human epithelium kidney 293T Lenti-X cells (Clontech Laboratories, CA, USA) were seeded on 100-mm-diameter Petri dishes and maintained in Dulbecco's modified Eagle's medium (Thermo Fisher, MA, USA) supplemented with 10% fetal bovine serum (GE Healthcare Life Sciences, HyClone Laboratories, South Logan, UT, USA) and 100 U/mL penicillin-streptomycin-glutamine (Thermo Fisher). Cells were transfected with 12 µg per plate of a plasmid mixture containing transfer vector, packaging plasmid, and VSV.G plasmid in a 6:4:2 ratio, using the JetPrime transfection kit (Polyplus Transfection, Illkirch, France) following the manufacturer's recommendations. At 48 and 72 h posttransfection, filtered supernatants were concentrated by ultracentrifugation for 2 h at 23,000 rpm on a 20% sucrose cushion. Pelleted vector particles were resuspended in 1× PBS and stored at -80°C . Each LV-GFP and IDLV-GFP stock was titrated using reverse transcriptase (RT) activity assay (RetroSys RT ELISA kit; Innogen,

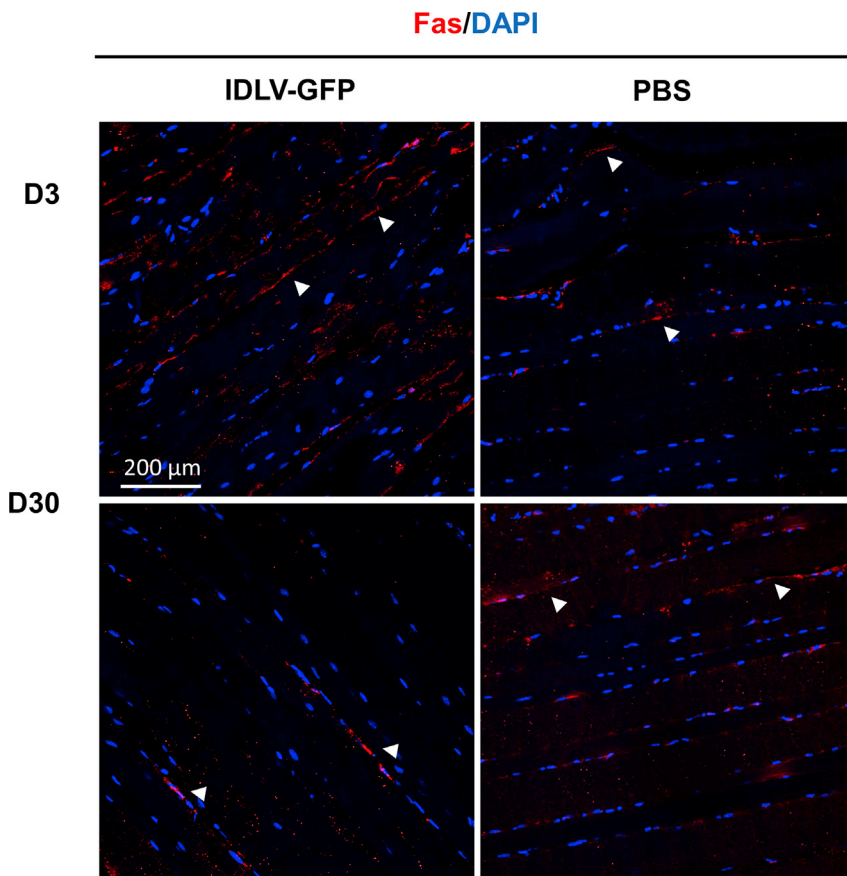


Figure 8. Fas Expression in Muscle Tissue Is Independent of Immunization

Muscle tissue harvested at 3 and 30 days after i.m. injection with IDLV-GFP or PBS was stained with anti-Fas antibody (red) and DAPI (blue). White arrowheads indicate Fas-expressing cells.

Immunofluorescence

Sections 8 μM thick were cut from OCT-embedded tissue blocks and placed on charged microscope slides for staining. Slides were blocked for 60 min using 10% serum with 0.03% Triton X-100 (Thermo Fisher) in 1 \times PBS. For immunofluorescence staining of primary myoblasts and myocytes, cells were incubated on well chamber slides and fixed with 4% paraformaldehyde in 1 \times PBS. Subsequently, endogenous biotin was blocked using a biotin/streptavidin blocking kit according to the manufacturers' instructions (SP-2002; Vector Lab, CA, USA). Antibodies were diluted in 1% BSA (A7906; Sigma) and 0.03% Triton X-100 (staining/wash buffer). Primary antibodies, including anti-GFP (Ab6556; Abcam, Cambridge, UK), anti-beta-spectrin (2808; Abcam), Biotin anti-H2Kd (BD553564; BD, NJ, USA), or anti-Fas (82419; Abcam) were added at a 1:200 dilution. Slides were placed in a humidified chamber and incubated overnight at 4°C. After three washes with staining/wash buffer, Alexa Fluor

Lund, Sweden), and the corresponding transducing units (TUs) calculated by comparing the RT activity with the infectious titers in 293T Lenti-X cells.

Animals and Immunization Protocols

Female BALB/c mice 4–7 weeks of age were purchased from Charles River Laboratories and housed in the Duke University Regional Biocontainment Laboratory facilities. All animal procedures were approved by the Institutional Animal Care and Use Committee (IACUC) prior to the experiments. Animals were housed and cared for according to local, state, and federal policies in an Association for Assessment and Accreditation of Laboratory Animal Care International (AAALAC)-accredited facility. Groups of four mice were injected with 5×10^6 TUs of IDLV-GFP or PBS in a final volume of 100 μL (50 $\mu\text{L}/\text{leg}$) either i.m. in the calf muscles or s.c. under the skin surrounding the calf muscles. Groups of four naive mice were kept untreated as negative controls. At the indicated time points, mice were sacrificed by CO₂ inhalation, and spleen, muscle, skin, and dLNs were harvested and processed. Injection sites were excised from the mice and fixed for 24 h in neutral-buffered formalin followed by either routine paraffin embedding or freezing in Tissue-Tek OCT medium (VWR, PA, USA) in an LN₂-cooled isopentane bath (Sigma, St. Louis, MO, USA).

488 (Abcam), Alexa Fluor 594 (Abcam), and Streptavidin Alexa Fluor 594 (Thermo Fisher) secondary antibodies (Abcam) were added and incubated for 1 h in the dark at room temperature. DAPI (Invitrogen, CA, USA) was used to visualize nuclei. Coverslips were mounted using Prolong Gold Antifade Mountant (Thermo Fisher) and allowed to cure in the dark for up to 24 h. Slides were then imaged on a Zeiss LSM 510 Confocal microscope. ImageJ software (NIH) was used for expression quantification.

Histology and Immunohistochemistry

To analyze the cellular infiltration, 5- μM -thick sections were cut from paraffin-embedded tissue blocks and placed on charged microscope slides for staining. Sections were deparaffinized, rehydrated, and subjected to routine hematoxylin (Sigma) and eosin (Sigma) staining. Representative images were acquired using a Zeiss AxioImager microscope. To determine the phenotype of the cells at the injection site, 5- μM sections from paraffin-embedded tissues were cut, prepared, and blocked as described above. Endogenous peroxidase/phosphatase activity was blocked using Bloxall reagent (Vector Labs). Anti-F4/80 (6640; Abcam) and anti-CD3 (RM-9107; Thermo Scientific) as primary antibodies and horseradish peroxidase (HRP)-conjugated secondary antibodies were used. Peroxidase activity was visualized using NovaRed HRP substrate (Vector Labs). Slides were then

counterstained with hematoxylin, dehydrated with ethanol, and cleared with xylene substitute (Sigma). Coverslips were mounted with Organo/Limonene mounting medium (Sigma). Representative images were acquired using a Zeiss AxioImager microscope.

IFN γ ELISpot Assay

Spleens harvested from each mouse at the time of euthanasia were homogenized using an Eppendorf pestle and passed through a 100- μ m filter cell strainer (BD) to obtain single-cell suspensions. Red cells were lysed using Red Blood Cell Lysis Buffer (Sigma) according to the manufacturers' instructions. After washing, cells were resuspended in RPMI 1640 medium (Thermo Fisher) supplemented with 10% FBS (Sigma), 2 mM L-glutamine, 1% penicillin/streptomycin (Sigma), and 50 mM 2-mercaptoethanol (Sigma). Cell viability was assessed by trypan blue (Invitrogen) exclusion. Cells were seeded at 200,000 viable cells per well into polyvinylidene fluoride (PVDF) 96-well plates coated with anti-mouse IFN- γ antibody (Mouse IFN- γ ELISpot; BD). IFN- γ detection was performed according to the manufacturer's instructions. The H-2Kd-restricted GFP 9-mer peptide HYLSTQSAL (2 μ g/mL; Proimmune, UK) was used to quantify antigen-specific IFN- γ -producing cells. Concanavalin A (10 μ g/mL; Sigma) was used as a positive control. MHC class I (H-2Kd/H-2Dd) monoclonal antibody (Thermo Fisher) was used to block MHC class I molecules. NovaRed HRP substrate was used to visualize spots. Spots were counted using ImmunoSpot Analyzer (ImmunoSpot). Data are expressed as GFP-specific SFCs per million cells and as a ratio between GFP and ConA SFCs \times 100 (%). A positive response was at least a 2-fold increase of spots over medium-treated wells (background) with minimum threshold of 50 SFCs per million cells in the stimulated wells.

Generation of Primary Murine Myoblasts and Myocytes

Muscle satellite cells were isolated using a previously described protocol⁴⁴ with minor modifications. In brief, thigh muscles were harvested from 3-week-old BALB/c female mice. After chopping muscle into 1-mm-diameter pieces, tissue was digested by collagenase II (Sigma) for 30 min at 37°C, ground through 70- μ m filters (BD) to remove large pieces, and seeded on 10% Matrigel pre-coated plates. After 72 h, cells were detached with 0.25% trypsin-EDTA and seeded on uncoated culture plates for 45 min at 37°C to allow large cells, including fibroblasts, to adhere. Supernatants containing myoblasts that did not adhere to the plate were then collected and seeded onto 10% Matrigel pre-coated plates. Myoblasts were maintained either in culture medium, F-10 (GIBCO, MA, USA) containing 20% FBS (GIBCO), 2.5 ng/mL human FGF recombinant protein (Thermo Fisher), and 0.2% chicken embryo extraction (Gemini 100-163P) or differentiated into myocytes using a differentiation medium containing DMEM (GIBCO), 2% horse serum (HyClone, IL, USA), and 4 μ M human insulin (Sigma) for 5–7 days.

Transduction with LV-GFP and Flow Cytometry Analysis

Primary myoblasts were transduced with LV-GFP or LV-Fas/GFP (multiplicity of infection of 5) in culture medium. After 3 days, cells were washed and either maintained in myoblast culture medium or

differentiated into myocytes as described above. GFP expression was assessed by fluorescent microscopy or flow cytometry using an LSRII flow cytometer (BD), and results were analyzed using FlowJo software (Tree Star).

Expression of Fas was assessed by flow cytometry after staining with anti-Fas-PE-Cy7 (Jo2; BD) for 30 min at 4°C in PBS containing 3% FBS and 10 mM EDTA (Sigma). Dead cells were positively stained with LIVE/DEAD Fixable Aqua Dead Cell Stains (Molecular Probes, OR, USA) or LIVE/DEAD Fixable Far Red Dead Cell Stains (Invitrogen, CA, USA). Isotype control antibodies were used as negative controls.

LDH Cytotoxicity Assay

Splenocytes purified from IDLV-GFP-immunized mice were seeded in 24-well plates at 1×10^6 /mL and activated with the H-2Kd-restricted 9-mer GFP peptide (10 μ g/mL) for 3 days. Primary myoblasts and myocytes were pulsed with GFP peptide (5 μ g/mL) for 2 h and then co-cultured with activated splenocytes (effector cells) at different effector-to-target (E:T) cell ratios. The murine cell line P815 (ATCC:TIB-64) was used as a positive control for the assay. After 6 and 8 h of incubation, supernatants were collected, and the release of LDH was measured using the LDH cytotoxicity assay kit (Thermo Fisher) according to the manufacturer's instructions. The % cytotoxicity for each E:T cell ratio was calculated using the following formula: % Cytotoxicity = (experimental value – effector cells spontaneous control – target cells spontaneous control)/(target cell maximum control – target cells spontaneous control) \times 100.

FasL-Induced Cytotoxicity Assay

Primary myoblasts and myocytes were treated overnight with recombinant mouse FasL-His Tag (526-SA; R&D Systems, MN, USA) protein at different concentrations ranging from 0 to 2 μ g/mL either in complete culture medium or in serum-free medium, containing 10 μ g/mL anti-His-Tag antibody (MA1-135; Thermo Fisher). Splenocytes from naive BALB/c mice were used as a positive control of FasL-induced cytotoxicity. Dead cells were counted after trypan blue staining. Cells cultured without FasL were used as control of the assay. The % cytotoxicity was calculated using the following equation:

$$\% \text{ Cytotoxicity} = \frac{(\text{Number of dead cells} - \text{Number of dead cells in control sample})}{(\text{Total cell number} - \text{Number of dead cells in control sample})} \times 100$$

The FasL-mediated cell death in myoblasts transduced with LV-GFP and LV-Fas/GFP was evaluated by flow cytometry with LIVE/DEAD Fixable Far Red Dead Cell Stains (Invitrogen, CA, USA), gating on the GFP⁺ or GFP⁻ populations.

Statistical Analyses

The magnitude and durability of immune responses in the different immunization groups were compared using two linear regression models, one for GFP-specific T cell responses and another for the SFC ratio between GFP and ConA. The GFP-specific T cell responses

were natural log transformed, and the SFC ratio between GFP and ConA was arcsine transformed. There were no adjustments made to the alpha level for multiple comparison; thus, p values <0.05 were considered significant.

AUTHOR CONTRIBUTIONS

Y.-Y.L. participated in the study design, performed the majority of the experiments, analyzed the data, and wrote the manuscript. I.B. performed part of the experiments and analyzed the data. M.B. oversaw vector production for *in vitro* and *in vivo* experiments, and contributed to study design, data analysis, and editing of the manuscript. M.-N.H. performed flow cytometry experiments and analyzed the data. A.F.B. provided input and supervised the immunohistochemistry (IHC) and immunofluorescence (IF) experiments, analyzed the data, and edited the manuscript. W.R. performed statistical analyses. M.E.K. provided input on study design, planning of experiments, interpretation of the data, and editing of the manuscript. D.N. and A.C. oversaw the planning and direction of the project, including analysis and interpretation of the data and editing of the manuscript.

CONFLICTS OF INTEREST

The authors declare no competing interests.

ACKNOWLEDGMENTS

The authors thank Kris Riebe and Gregory Sempowski for their support with mouse immunization and sampling, Deborah Pajalunga for providing the protocol for purification and differentiation of myoblasts, and Bala Balakumaran for his help with study coordination. Animal studies were done in the Duke Regional Biocontainment Laboratory, which received partial support for construction from the National Institutes of Health, National Institute of Allergy and Infectious Diseases (UC6-AI058607). This work was supported by National Institute of Allergy and Infectious Diseases (NIAID) 1P01AI110485-01A1 to M.E.K. This publication resulted in part from research supported by the Duke University Center for AIDS Research (CFAR, NIH-funded program 5P30 AI064518) to M.B. This project has received funding from the European Union's Horizon 2020 research and innovation program under grant agreement no. 681137 (EAVI2020) and from the European Union's Seventh Programme for Research, Technological Development and Demonstration under grant agreement no. 280873 (ADITEC) to A.C. and D.N.

REFERENCES

- Plotkin, S.A. (2009). Vaccines: the fourth century. *Clin. Vaccine Immunol.* *16*, 1709–1719.
- Rodrigues, C.M.C., Pinto, M.V., Sadarangani, M., and Plotkin, S.A. (2017). Whither vaccines? *J. Infect.* *74* (Suppl 1), S2–S9.
- Liu, M.A. (2010). Gene-based vaccines: Recent developments. *Curr. Opin. Mol. Ther.* *12*, 86–93.
- Ewer, K.J., Lambe, T., Rollier, C.S., Spencer, A.J., Hill, A.V., and Dorrell, L. (2016). Viral vectors as vaccine platforms: from immunogenicity to impact. *Curr. Opin. Immunol.* *41*, 47–54.
- Rollier, C.S., Reyes-Sandoval, A., Cottingham, M.G., Ewer, K., and Hill, A.V. (2011). Viral vectors as vaccine platforms: deployment in sight. *Curr. Opin. Immunol.* *23*, 377–382.
- Coutant, F., Sanchez David, R.Y., Félix, T., Boulay, A., Caleechurn, L., Souque, P., Thouvenot, C., Bourgooin, C., Beignon, A.S., and Charneau, P. (2012). A nonintegrative lentiviral vector-based vaccine provides long-term sterile protection against malaria. *PLoS ONE* *7*, e48644.
- Méndez, A.C., Rodríguez-Rojas, C., and Del Val, M. (2019). Vaccine vectors: the bright side of cytomegalovirus. *Med. Microbiol. Immunol. (Berl.)* *208*, 349–363.
- Lundstrom, K. (2019). RNA Viruses as Tools in Gene Therapy and Vaccine Development. *Genes (Basel)* *10*, E189.
- Negri, D.R., Michelini, Z., and Cara, A. (2010). Toward integrase defective lentiviral vectors for genetic immunization. *Curr. HIV Res.* *8*, 274–281.
- Negri, D.R., Michelini, Z., Bona, R., Blasi, M., Filati, P., Leone, P., Rossi, A., Franco, M., and Cara, A. (2011). Integrase-defective lentiviral-vector-based vaccine: a new vector for induction of T cell immunity. *Expert Opin. Biol. Ther.* *11*, 739–750.
- Wanisch, K., and Yáñez-Muñoz, R.J. (2009). Integration-deficient lentiviral vectors: a slow coming of age. *Mol. Ther.* *17*, 1316–1332.
- Vargas, J., Jr., Gusella, G.L., Najfeld, V., Klotman, M.E., and Cara, A. (2004). Novel integrase-defective lentiviral episomal vectors for gene transfer. *Hum. Gene Ther.* *15*, 361–372.
- Gillim-Ross, L., Cara, A., and Klotman, M.E. (2005). HIV-1 extrachromosomal 2-LTR circular DNA is long-lived in human macrophages. *Viral Immunol.* *18*, 190–196.
- Apolonia, L., Waddington, S.N., Fernandes, C., Ward, N.J., Bouma, G., Blundell, M.P., Thrasher, A.J., Collins, M.K., and Philpott, N.J. (2007). Stable gene transfer to muscle using non-integrating lentiviral vectors. *Mol. Ther.* *15*, 1947–1954.
- Athanasopoulos, T., Munye, M.M., and Yáñez-Muñoz, R.J. (2017). Nonintegrating Gene Therapy Vectors. *Hematol. Oncol. Clin. North Am.* *31*, 753–770.
- Negri, D.R., Michelini, Z., Baroncelli, S., Spada, M., Vendetti, S., Buffa, V., Bona, R., Leone, P., Klotman, M.E., and Cara, A. (2007). Successful immunization with a single injection of non-integrating lentiviral vector. *Mol. Ther.* *15*, 1716–1723.
- Karwacz, K., Mukherjee, S., Apolonia, L., Blundell, M.P., Bouma, G., Escors, D., Collins, M.K., and Thrasher, A.J. (2009). Nonintegrating lentivector vaccines stimulate prolonged T-cell and antibody responses and are effective in tumor therapy. *J. Virol.* *83*, 3094–3103.
- Grasso, F., Negri, D.R., Mochi, S., Rossi, A., Cesolini, A., Giovannelli, A., Chiantore, M.V., Leone, P., Giorgi, C., and Cara, A. (2013). Successful therapeutic vaccination with integrase defective lentiviral vector expressing nononcogenic human papillomavirus E7 protein. *Int. J. Cancer* *132*, 335–344.
- Fontana, J.M., Christos, P.J., Michelini, Z., Negri, D., Cara, A., and Salvatore, M. (2014). Mucosal immunization with integrase-defective lentiviral vectors protects against influenza virus challenge in mice. *PLoS ONE* *9*, e97270.
- Negri, D., Blasi, M., LaBranche, C., Parks, R., Balachandran, H., Lifton, M., Shen, X., Denny, T., Ferrari, G., Vescio, M.F., et al. (2016). Immunization with an SIV-based IDLV Expressing HIV-1 Env 1086 Clade C Elicits Durable Humoral and Cellular Responses in Rhesus Macaques. *Mol. Ther.* *24*, 2021–2032.
- Blasi, M., Negri, D., LaBranche, C., Alam, S.M., Baker, E.J., Brunner, E.C., Gladden, M.A., Michelini, Z., Vandergrift, N.A., Wiehe, K.J., et al. (2018). IDLV-HIV-1 Env vaccination in non-human primates induces affinity maturation of antigen-specific memory B cells. *Commun. Biol.* *1*, 134.
- Somaiah, N., Block, M.S., Kim, J.W., Shapiro, G.I., Do, K.T., Hwu, P., Eder, J.P., Jones, R.L., Lu, H., Ter Meulen, J., et al. (2019). First-in-class, first-in-human study evaluating LV305, a dendritic-cell tropic lentiviral vector, in sarcoma and other solid tumors expressing NY-ESO-1. *Clin. Cancer Res.* *25*, 5808–5817.
- Michelini, Z., Negri, D.R., Baroncelli, S., Spada, M., Leone, P., Bona, R., Klotman, M.E., and Cara, A. (2009). Development and use of SIV-based Integrase defective lentiviral vector for immunization. *Vaccine* *27*, 4622–4629.
- Baumjohann, D., Preite, S., Reboldi, A., Ronchi, F., Ansel, K.M., Lanzavecchia, A., and Sallusto, F. (2013). Persistent antigen and germinal center B cells sustain T follicular helper cell responses and phenotype. *Immunity* *38*, 596–605.
- Quinn, K.M., Zak, D.E., Costa, A., Yamamoto, A., Kastenmuller, K., Hill, B.J., Lynn, G.M., Darrach, P.A., Lindsay, R.W., Wang, L., et al. (2015). Antigen expression

- determines adenoviral vaccine potency independent of IFN and STING signaling. *J. Clin. Invest.* *125*, 1129–1146.
26. Cousin, C., Oberkamp, M., Felix, T., Rosenbaum, P., Weil, R., Fabrega, S., Morante, V., Negri, D., Cara, A., Dadaglio, G., and Leclerc, C. (2019). Persistence of integrase-deficient lentiviral vectors correlates with the induction of STING-independent CD8⁺ T cell responses. *Cell Rep.* *26*, 1242–1257.e7.
 27. Rossi, A., Michelini, Z., Leone, P., Borghi, M., Blasi, M., Bona, R., Spada, M., Grasso, F., Gugliotta, A., Klotman, M.E., et al. (2014). Optimization of mucosal responses after intramuscular immunization with integrase defective lentiviral vector. *PLoS ONE* *9*, e107377.
 28. Kägi, D., Vignaux, F., Ledermann, B., Bürki, K., Depraetere, V., Nagata, S., Hengartner, H., and Golstein, P. (1994). Fas and perforin pathways as major mechanisms of T cell-mediated cytotoxicity. *Science* *265*, 528–530.
 29. Egeblad, M., and Jäättelä, M. (2000). Cell death induced by TNF or serum starvation is independent of ErbB receptor signaling in MCF-7 breast carcinoma cells. *Int. J. Cancer* *86*, 617–625.
 30. Braun, F., Bertin-Ciftci, J., Gallouet, A.S., Millour, J., and Juin, P. (2011). Serum-nutrient starvation induces cell death mediated by Bax and Puma that is counteracted by p21 and unmasked by Bcl-x(L) inhibition. *PLoS ONE* *6*, e23577.
 31. Hu, B., Dai, B., and Wang, P. (2010). Vaccines delivered by integration-deficient lentiviral vectors targeting dendritic cells induces strong antigen-specific immunity. *Vaccine* *28*, 6675–6683.
 32. Gallinaro, A., Borghi, M., Bona, R., Grasso, F., Calzoletti, L., Palladino, L., Cecchetti, S., Vescio, M.F., Macchia, D., Morante, V., et al. (2018). Integrase Defective Lentiviral Vector as a Vaccine Platform for Delivering Influenza Antigens. *Front. Immunol.* *9*, 171.
 33. Michelini, Z., Negri, D., and Cara, A. (2010). Integrase defective, nonintegrating lentiviral vectors. *Methods Mol. Biol.* *614*, 101–110.
 34. Albershardt, T.C., Campbell, D.J., Parsons, A.J., Slough, M.M., Ter Meulen, J., and Berglund, P. (2016). LV305, a dendritic cell-targeting integration-deficient ZVex(TM)-based lentiviral vector encoding NY-ESO-1, induces potent anti-tumor immune response. *Mol. Ther. Oncolytics* *3*, 16010.
 35. Worbs, T., Hammerschmidt, S.I., and Förster, R. (2017). Dendritic cell migration in health and disease. *Nat. Rev. Immunol.* *17*, 30–48.
 36. Nadafi, R., Koning, J.J., Veninga, H., Stachte, X.N., Konijn, T., Zwiers, A., Malmström, A., den Haan, J.M.M., Mebius, R.E., Maccarana, M., and Reijmers, R.M. (2018). Dendritic Cell Migration to Skin-Draining Lymph Nodes Is Controlled by Dermatan Sulfate and Determines Adaptive Immunity Magnitude. *Front. Immunol.* *9*, 206.
 37. Jiang, H., Wang, Q., and Sun, X. (2017). Lymph node targeting strategies to improve vaccination efficacy. *J. Control. Release* *267*, 47–56.
 38. Abbas, A., Lichtman, A.H., and Pillai, S. (2017). *Cellular and Molecular Immunology*, Ninth Edition (Elsevier).
 39. Wiendl, H., Hohlfeld, R., and Kieseier, B.C. (2005). Immunobiology of muscle: advances in understanding an immunological microenvironment. *Trends Immunol.* *26*, 373–380.
 40. Nagaraju, K., Raben, N., Loeffler, L., Parker, T., Rochon, P.J., Lee, E., Danning, C., Wada, R., Thompson, C., Bahtiyar, G., et al. (2000). Conditional up-regulation of MHC class I in skeletal muscle leads to self-sustaining autoimmune myositis and myositis-specific autoantibodies. *Proc. Natl. Acad. Sci. USA* *97*, 9209–9214.
 41. Afzali, A.M., Müntefering, T., Wiendl, H., Meuth, S.G., and Ruck, T. (2018). Skeletal muscle cells actively shape (auto)immune responses. *Autoimmun. Rev.* *17*, 518–529.
 42. Hassin, D., Garber, O.G., Meiraz, A., Schiffenbauer, Y.S., and Berke, G. (2011). Cytotoxic T lymphocyte perforin and Fas ligand working in concert even when Fas ligand lytic action is still not detectable. *Immunology* *133*, 190–196.
 43. Kang, S.M., Hoffmann, A., Le, D., Springer, M.L., Stock, P.G., and Blau, H.M. (1997). Immune response and myoblasts that express Fas ligand. *Science* *278*, 1322–1324.
 44. Pajalunga, D., Franzolin, E., Stevanoni, M., Zribi, S., Passaro, N., Gurtner, A., Donsante, S., Loffredo, D., Losanno, L., Bianchi, V., et al. (2017). A defective dNTP pool hinders DNA replication in cell cycle-reactivated terminally differentiated muscle cells. *Cell Death Differ.* *24*, 774–784.